Supporting Information

Doubling Reversible Capacities in Epitaxial $Li_4Ti_5O_{12}$ Thin Film Anodes for Microbatteries

*Daniel M. Cunha[1], Theodoor A. Hendriks[1], Alexandros Vasileiadis[2], Chris M. Vos[1], Tomas Verhallen[2], Deepak P. Singh[1], Marnix Wagemaker[2] and Mark Huijben[1]**

[1] MESA+ Institute for Nanotechnology, University of Twente, 7500 AE, Enschede, Netherlands.
[2] Faculty of Applied Sciences, Technical University Delft, 2629 JB, Delft, Netherlands.
*m.huijben@utwente.nl

A. Phase Field Simulations

All the thermodynamic and kinetic parameters implemented in the phase field model are based on literature. Argumentation upon the parameter selection is established in the study of Vasileiadis et al.[1] where the phase field model is presented in detail.

Table S1: Thermodynamic and kinetic parameters implemented in the phase field model

Thermodynamic Parameters	Value	Based on
Enthalpy of Mixing (Ω_a)	$1.43 \cdot 10^{-20}$ J/Li	DFT
Gradient Penalty (κ)	$1 \cdot 10^{-10}$ J/m	TEM, DFT
Equilibrium potential (μ^{Θ})	1.55 V	Electrochemical experiments
LTO density (ϱ_{LTO})	3.5 g/cm^3	
Kinetic Parameters		
Li-ion Diffusivity (D_{Li})	$4 \cdot 10^{-16}$ m^2/s	NMR
Electronic Conductivity (σ)	10 S/m	Electrochemical experiments
Electrolyte Anion Diffusion	$2.94 \cdot 10^{-10}$ m^2/s	Commercial LiPF6 EC/DMC
Electrolyte Cation Diffusion	$2.2 \cdot 10^{-10}$ m^2/s	Commercial LiPF6 EC/DMC
Reaction Rate Constant (k_0)	3.6 A/m^2	Electrochemical experiments

The geometrical parameters of the thin film batteries are presented below. The batteries have well determined thicknesses, porosity and separator characteristics. In addition, the absence of pores makes it clear that the diffusion coordinate in the solid particles/grains will be comparable to the thickness of the electrode.

Table S2: Geometrical parameters implemented in the phase field model

Geometry Parameters		
Electrode Thickness	55/110/220/330 nm	SEM images, epitaxial technique
Particle Morphology	**grains visible**	**SEM images**
Particle Radius (R)	**55/110/220/330 nm**	**equal to film thickness**
Electrode porosity (ε)	0.5%	SEM images, epitaxial technique
Separator Length (L_s)	25 µm	Celgard
Separator Porosity (ε_s)	55 %	Celgrad
LTO Volume Loading (PL_c)	99.5 %	Synthesis process

The only parameter that needs to be investigated with the simulation technique is the grain size. Additionally, we need to investigate how the grain boundaries will affect the lithiation process. This is because the presence of grain boundaries is expected to enhance diffusion[1-4] by breaking the core-shell symmetry, possibly creating more phase interfaces.[2] The phase field model was designed to capture spherical or cylindrical particles in electrolyte bath. For the thin film case, however, these particle shapes will overestimate lithiation (the absence of pores indicates that electrolyte does not wet the whole surface of the particle but rather the front side of the film). On the other hand, considering that the LTO grains lithiate strictly from one direction (rectangular shaped particles with only one side active) is likely to underestimate lithiation as it completely ignores the effect of grain boundaries and the existence of multiple phase fronts. The volume fractions with respect the diffusion length in the solid particle of the different particle descriptions are presented in **Figure S1**. It can be observed that lithiating the outer part of a spherical particle accounts of a much larger volume fraction of the whole particle than the inner part while in the one-way-rectangular description the volume fractions throughout the particle are the same.

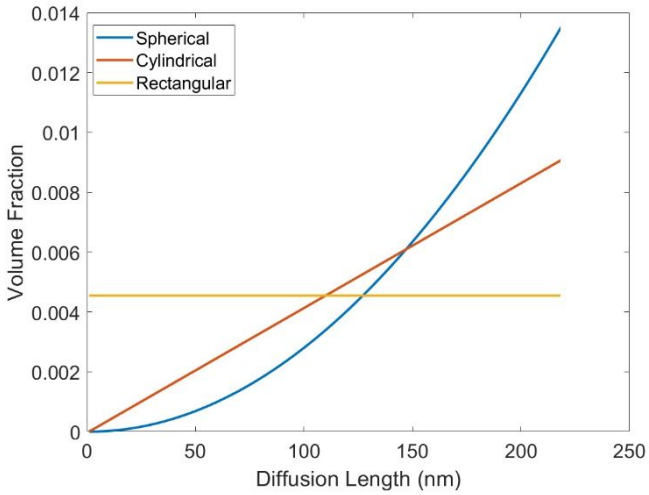

Figure S1: Volume fractions vs. diffusion length of three particle shapes for a 220nm particle. The 0 nm marks the end/center of the particle. The rectangular description refers to a strictly one-direction lithiation wave (only one side of the rectangular is considered active).

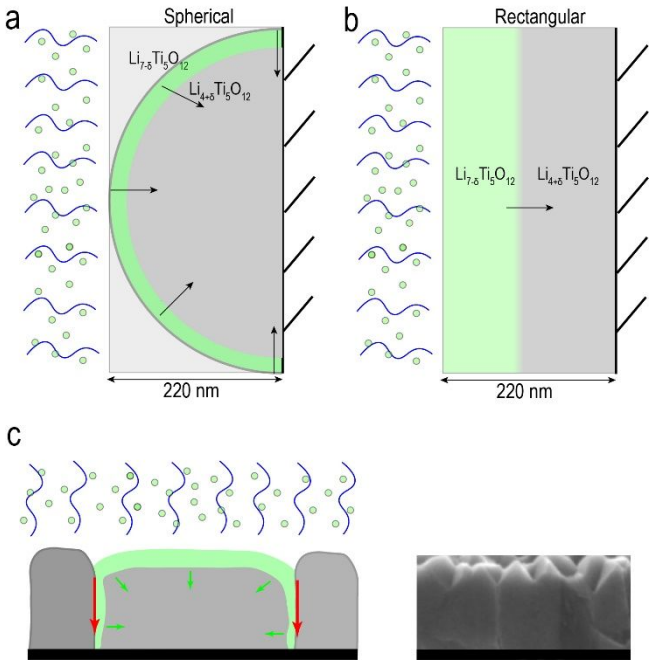

Figure S2: The two-phase lithiation mechanism for a) spherical approximation and b) single-direction rectangular approximation. When we are referring to single-direction rectangular approximation we are considering that only one side (the one exposed to the electrolyte) is active c) example of grain boundary behavior and lithiation of a grain of the thin film in comparison with a zoomed-in SEM image of the film.

The approximations we mentioned above are schematically presented in **Figure S2a and b**. Initially, for simplicity we assumed the grains to be particles with the diffusion direction equal to the length of the thin film in order to see which description produces the best match. The results are presented in **Figure S3a, b and c**. The experimentally determined bulk capacities (1.5-1.6V) are compared with the simulation results for spherical, cylindrical and one-way-rectangular particle shapes respectively for all film thicknesses and currents. The spherical approximation shows the best trend behavior, matching the shape of the decreasing capacity staircase. Good agreement is observed for the thicker films. For the 55 and 110 nm films the difference is larger as the simulated results converge faster to the maximum theoretical capacity. The single-direction rectangular approximation, that initially seems more logical for the thin film batteries, shows an extremely steep decrease in capacity with increasing thickness. This indicates that the propagating lithiation wave is not single directional and uniform but at least part of the lithiation occurs with radial-like conditions. The only way to achieve this in the zero-porosity system is by the catalytic role of grain boundaries. The proposed mechanism of a more radial-like lithiation process is presented in **Figure S2c**. The grain boundaries lead to Li-poor and Li-rich phase-interfaces, along which fast diffusion occurs allowing the bulk lithiation wave (or waves in-case of multiple phase-fronts) to propagate inwards in a radial-like manner.

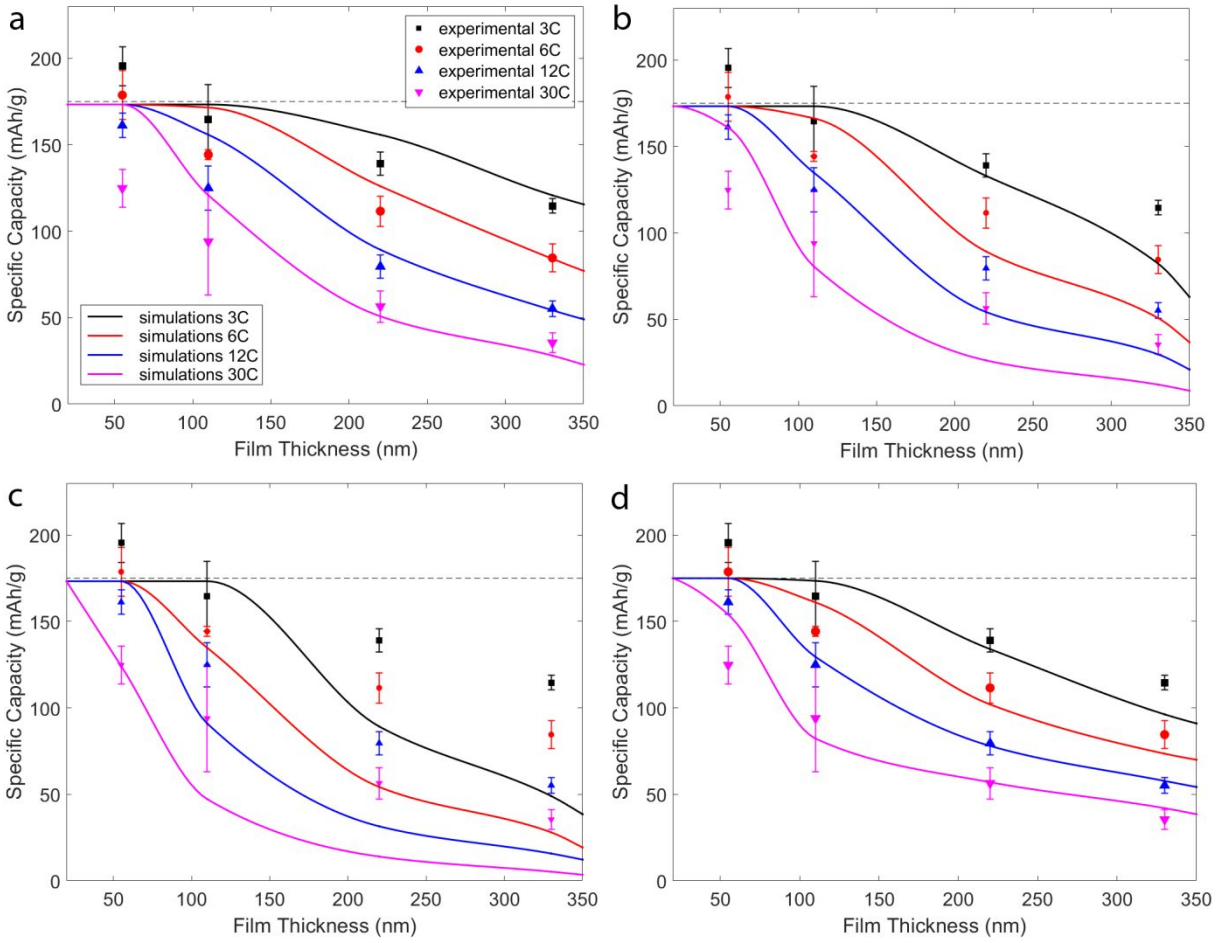

Figure S3: Experimental (scatter) vs. simulated (lines) results for the a) spherical b) cylindrical and c) single-direction rectangular approximations. d) experimental p(scatter) vs. simulated (lines) results. The grains of the films were assumed to be lithiated part with the radial approximation and part with the single-direction approximation.

Further, we performed simulations of all 3 particle approximations with different (larger and smaller) diffusion coefficients in order to examine how it affects the results. For example, choosing a much higher diffusion coefficient for the single-direction rectangular approximation might lead to accurate reproduction of the experimental trend. However, our findings suggest that this is not the case. Simply by tuning the diffusion coefficient cannot capture the shape of the experimental trend, indicating that our interpretation (presented in the previous paragraph) is not affected by the choice of diffusion coefficient. In addition, implementing different diffusion coefficients in order to match the experimental results gives an artificial character to the description. Staying close to measured, with direct methods such as nuclear magnetic resonance (NMR), diffusion coefficients is important for a physical and not artificial description.

In reality, a mixed behavior is expected. Part of the grain should feel radial-like conditions, while grain shapes with one dimension much larger than the other should also fall under the single-direction rectangular approximation description after a certain point. This is the reason why the spherical description overestimates greatly the 55 and 110 nm films. It is likely that the grain length on the horizontal to the film dimension might be larger than the 55 nm so that the film thickness is far from to be considered a radius and the radial-like lithiation falls apart to rectangular in some parts of the grain (**Figure S2c)**. In order to test that we are thinking towards the right direction, we performed computations breaking the grain into two shapes. 10 – 25%

of the particle was considered with radial-like conditions (to capture the grain boundary enhancement) and 90 – 75% of the particle with one-way-rectangular conditions (which is logically expected in a film description). The results are presented in **Figure S3d**. We can clearly see that with this very simple treatment, the trend lines remained true to the experimental shape but now the thinner films are described much better as well. This explains the capacity loss that is observed for the small thicknesses experimentally.

The observed experimental trend lines are the result of many parameters (Li-transport resistances, electronic conductivity etc.) so that coming to conclusions for the solid diffusion and grain effects is difficult. However, the thin films offers us an advantage of having very well determined parameters, being ideal for simulations. The absence of pores indicates that the transport properties are limited in the separator. In addition, the limited thickness of the film hints that electronic conductivity would play an insignificant role. This has been demonstrated for systems even at the microscale, taking advantage of the tremendous enhancement of LTO electronic properties once Li-ions start being inserted.[1, 5] The above statements were tested in detail with the phase field model. We analyzed all the contributions of the various kinetic mechanisms to the total overpotential in order to determine the rate limiting mechanism of the thin film batteries. In **Figure S4** the overpotential contributions of the 220nm film are presented, as an example, for the highest rate (30C). The model indicates that the thin films batteries are limited by solid diffusion and this is independent of the particle description. Thus, we can examine the observed capacity trends as the result of only Li-ion diffusion limitations, strengthening our conclusions about grain boundaries and solid diffusion. The overpotential analysis, also, reasons the observed bulk experimental capacity and its rate limiting mechanism.

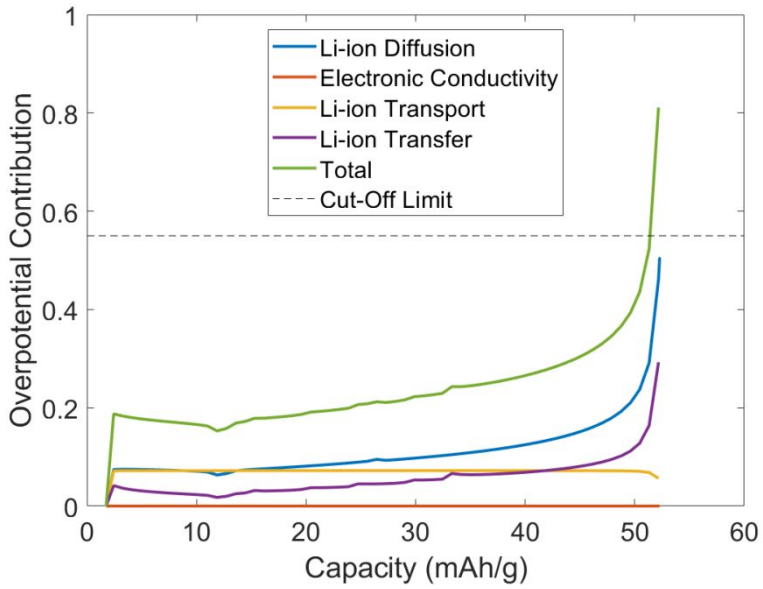

Figure S4: Overpotential analysis of the largest rate (30C) of the 220nm thin film. When the total overpotential reaches 0.55 V the cut-off is reached.

The information obtained from the above investigation is very important to understand the LTO grain boundary behavior and is relevant also for other electrode materials. An exact description, expanding further our phase field model, should include two separate effects, the fast grain boundary diffusion (red arrows in **Figure S2c)** and the two-phase lithium propagation in the

bulk (green arrows in **Figure S2c**). In addition, determining the grain size is of great importance as it will lead in an accurate description for the diffusion length in the solid that would require a, at least, 2D model description. Even though the above goals, exceed the scope of this paper, it sets a strong direction for explaining the effect of grain boundaries in LTO. Herein we focus on capturing the downward capacity trend observed experimentally and confirm the bulk measured capacities (capacities measured within the 1.5- 1.6 V voltage range). The model can accurately describe and provide insight on how to improve the thin film batteries. This is done assuming very simple approximations in 1D and implementing measured parameters.

B. References

1. Vasileiadis, A.; de Klerk, N. J. J.; Smith, R. B.; Ganapathy, S.; Harks, P. P. R. M. L.; Bazant, M. Z.; Wagemaker, M., Toward Optimal Performance and In-Depth Understanding of Spinel $Li_4Ti_5O_{12}$ Electrodes through Phase Field Modeling. *Adv. Funct. Mater.* **2018,** 28, 1705992.

2. Ganapathy, S.; Vasileiadis, A.; Heringa, J. R.; Wagemaker, M., The Fine Line between a Two-Phase and Solid-Solution Phase Transformation and Highly Mobile Phase Interfaces in Spinel $Li_{4+x}Ti_5O_{12}$. *Adv. Energy Mater.* **2017,** 7, 1601781.

3. Wang, C.; Wang, S. A.; He, Y. B.; Tang, L. K.; Han, C. P.; Yang, C.; Wagemaker, M.; Li, B. H.; Yang, Q. H.; Kim, J. K.; Kang, F. Y., Combining Fast Li-Ion Battery Cycling with Large Volumetric Energy Density: Grain Boundary Induced High Electronic and Ionic Conductivity in $Li_4Ti_5O_{12}$ Spheres of Densely Packed Nanocrystallites. *Chem. Mater.* **2015,** 27, 5647-5656.

4. Zhao, B.; Ran, R.; Liu, M. L.; Shao, Z. P., A comprehensive review of $Li_4Ti_5O_{12}$-based electrodes for lithium-ion batteries: The latest advancements and future perspectives. *Mat. Sci. Eng. R.* **2015,** 98, 1-71.

5. Song, M. S.; Benayad, A.; Choi, Y. M.; Park, K. S., Does $Li_4Ti_5O_{12}$ need carbon in lithium ion batteries? Carbon-free electrode with exceptionally high electrode capacity. *Chem. Commun.* **2012,** 48, 516-518.